

# Convection of a van der Waals fluid near the critical point

Henrik B. van Lengerich

---

## Abstract

Convection in a van der Waals fluid, with no-stress and fixed flux boundary conditions is studied. The problem is scaled with the infinite wavelength of the convection cell. A criterium is found that predicts the onset of convection; it contains information from the Rayleigh and Scharzschild criteria over the entire cell. The criterium is evaluated and compared with previous experiments on a similar experiment. Governing equations, boundary conditions, constitutive equation and convection mechanisms are explained.

---

## 1. Introduction

Past studies of convection have focused on incompressible or ideal gas fluids. The aim of this study is to approach a theory of convection for a fluid containing both a liquid and a gas phase. This is done by focusing on the conditions where the phase change originates, namely, the critical point of the substance.

Convection near the critical point is difficult both experimentally and theoretically because the fluctuation in properties becomes very large and many thermodynamic properties (such as the heat capacities and thermal conductivity) diverge. We model the fluid as an ideal van der Waals fluid, which a good qualitative (but not quantitative) model because it captures two phases, the critical point, and the divergence of thermodynamic properties. Because the thermal conductivity goes to infinity as the critical point is approached, we show that a fixed flux, rather than a fixed temperature boundary is appropriate. By doing this we can find the critical temperature difference by scaling the problem appropriately as done in [8].

This paper will first explain some of the previous research that has been done on convection near the critical point of the fluid. Background information is given to explain the properties of the van der Waals fluid and the onset of convection for both incompressible and compressible fluids. Finally, governing equations are derived for the situation to be studied, these equations are scaled, and then the criterion for the onset of convection is found.

## 2. Literature Review

The criterium for instability as well as the plan form function (the function which explains patterns and evolution) for an ideal gas with fixed flux and no-stress boundary conditions are described in [8]. Analysis of an incompressible fluid with no flux boundaries was done by Chapman and Proctor [7]. A derivation of when to use the constant flux condition was Hurle [11], however, this paper has a number of errors in it, of which the most crucial is that the thermal diffusivity and not thermal conductance was used to match the fluxes in the solid and fluid. This error is corrected in the boundary condition derivation in this report.

Experimental studies have been done by Kogan [12] to determine the onset of convection for  ${}^3\text{He}$  near the critical point. These find that the onset can be understood using only the Rayleigh criteria and the adiabatic temperature gradient (aka Schwarzschild criterion), the same result was found by Carles and Ugurtas [6] using the full governing equations and real data to determine which terms can be ignored. Experimental studies by Assenheimer [2] show that close to the critical point hexagons, lines, roll patches, and target or spiral patterns can be seen. This motivates the current research because it may be possible that additional patterns can be formed, and a plan form function of a van der Waals fluid would help to find the proper parameter regime.

Previous studies of convection near the critical point have focused on the "piston effect" which is the heating up of fluid close to the boundary, then the boundary fluid expands and compresses the bulk fluid, and the compression of the bulk fluid raises the bulk temperature. This was explained using thermodynamic arguments by Onuki [13] and then later derived by Pierre Carles in a lengthy manner using all the governing equations [9], [5]. Further studies continue to look at this piston effect [1], and in this authors opinion it is really boring because all that is done is the temperature of the walls is increased and then the fluid temperature increases; there is really nothing new here.

There have been some numerical simulations of van der Waals fluids close to the critical point [1], [15] but as mentioned before, these focus on the piston effect and do little in the way of making new predictions.

Lastly, there is a very good review of hydrodynamics near the critical point by Gitterman [10], and the thermodynamics for phase changes and close to the critical point are concisely explained in the second edition of Callen's book on thermodynamics [4].

### 3. Gas Properties

A typical phase diagram is shown in Figure 1. The liquid and gas are separated by a phase transition line. When the phase transition line is crossed there is a discontinuous jump in the thermodynamic properties of the fluid (such as conductivity, density, and heat capacity). This jump becomes smaller and smaller as one moves to higher temperature and pressure, until the discontinuities disappear at the critical point, which is where the line ends. Incidentally, no critical point has been found for the liquid-solid phase transition.

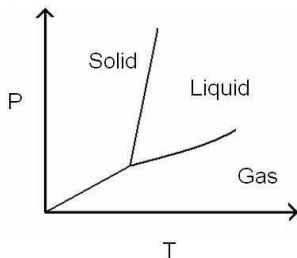


Fig. 1. Typical Phase Diagram

#### 3.1. Van der Waals Fluid

A van der Waals fluid is a bunch of particles that are attracted to each other by some potential effects and repelled due to a hard spheres shell. We assume that the attraction force decays to the -6 power. The constitutive equation

$$P = \frac{\mathfrak{R}\rho T}{1 - b\rho} - a\rho^2 \quad (1)$$

can be derived from such a model. Here  $b$  contains the information of the finite size of the particles, and as the density of the particles goes to  $1/b$  the space is completely packed with particles so the pressure goes to infinity. The  $a\rho^2$  term represents the attraction of the particles, and this tends to decrease the pressure.

In figure 2 are shown several isotherms of the van der Waals equation. The bottom (green) curve has an isotherm temperature below the critical point, from the phase diagram this suggests that the fluid has two phases. Where are the two phases? Imagine a fluid that lies on the green isotherm that has a density of about one, so that the slope is positive. Imagine a fluid blob at this point in a bunch of surrounding fluid. If the volume of this blob is made to be slightly bigger, then the pressure increases, so the volume continues to increase until the slope of the curve is negative. Similarly, if the volume is perturbed to be slightly smaller, the blob will continue to decrease in size until it reaches a point where the slope of the curve is negative. So all of the liquid will break up into high density and low density blobs, and these are the two phases. Usually a straight line is drawn across such there are no unstable slopes in the isotherm pressures, when this is done, it is easy to see the discontinuity in density that occurs at the phase transition. When the temperature is well beyond the critical value the top (red) curve shown in Figure 2 applies. This fluid has no phase transition because there are no parts with positive slopes. The middle curve is the curve at the critical temperature, the critical point is where the first and second derivatives of the pressure with respect to volume occur at the same volumes ( $\rho_c = \frac{1}{3b}, T_c = \frac{8a}{27b}, P_c = \frac{a}{27b^2}$ ).

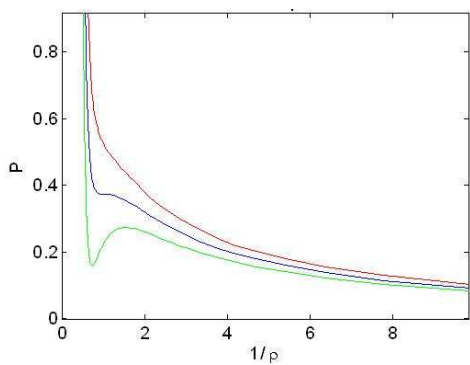


Fig. 2. Pressure for various isotherms

### 3.2. Diverging Properties near the Critical Point

By definition of an ideal van der Waals fluid the constant volume heat capacity is only a function of volume and does not diverge at the critical point. The constant pressure heat capacity can be found from the standard thermodynamic relation

$$C_P = C_V - \frac{T}{\rho^2} \left( \frac{\partial \rho}{\partial T} \right)_P \left( \frac{\partial P}{\partial T} \right)_\rho \quad (2)$$

$$C_P = C_V - \frac{T}{\rho^2} \frac{1}{\left( \frac{\partial T}{\partial \rho} \right)_P} \frac{\rho}{1 - b\rho} \quad (3)$$

$$C_P = C_V - \frac{\frac{8a}{27b}}{2a\frac{1}{3b}(1 - 1/3)^2 - \frac{8a}{27b}} \quad (4)$$

Where the last step was just inserting the critical values. The constant pressure heat capacity diverges the the -1 power as the critical point is approached. The thermal conductivity diverges to the roughly -1/2 power as shown in [14].

## 4. Convection Mechanisms

The criterium that determine the onset of convection can be derived from physical arguments. For an incompressible fluid the usual Rayleigh criteria is found. For a compressible fluid the adiabatic temperature gradient (or Schwarzschild criterium) is found.

### 4.1. Incompressible Convection

Consider a fluid blob of volume  $V = a^3$  contained in the fluid. Perturb the blob upward slightly, now it has a force directed upward due to the buoyancy and a force directed downward due to the viscous drag. Write the buoyancy force as

$$F_B = gV\delta\rho \quad (5)$$

The change in density is assumed to be due only due to the gradient in temperature

$$\delta\rho = -\rho\alpha\delta T \quad (6)$$

$$\alpha = -\frac{1}{\rho} \left( \frac{\partial\rho}{\partial T} \right)_P \quad (7)$$

The change in temperature of the blob is due to the temperature of the surroundings changing at a rate proportional to the temperature gradient times the rate at which this temperature diffuses into the blob.

$$\delta T = \frac{\Delta T}{d} v_z C_2 \frac{a^2}{\kappa} \quad (8)$$

This makes the buoyancy force equal to

$$F_B = -g\rho\alpha a^5 C_2 \frac{\Delta T}{d\kappa} v_z \quad (9)$$

The drag force is given by

$$F_D = C_1 a \mu v_z \quad (10)$$

By Newton's second law, the particle is stationary if the drag force is greater than the buoyancy force.

$$F_D > F_B \quad (11)$$

$$C_1 a \mu v_z > g\rho\alpha a^5 C_2 \frac{\Delta T}{d\kappa} v_z \quad (12)$$

$$a = C_3 d \quad (13)$$

$$\frac{C_1}{C_2 C_3^4} > \frac{g\alpha d^3 \Delta T}{\nu\kappa} \quad (14)$$

$$Ra_c > \frac{g\alpha d^3 \Delta T}{\nu\kappa} \quad (15)$$

This means that the fluid is stable if the Rayleigh number is below some critical Rayleigh number value.

### 4.2. Compressible Convection

Consider again a blob of fluid in its surrounding fluid. The blob has a density  $\rho_{blob}$  and the bulk fluid has an equal density  $\rho$ . Perturb the fluid upward slightly, now the blob has a density  $\rho_{blob} + \delta\rho_{blob}$  and the fluid has a density  $\rho(z + \delta z)$ . The force on the particle at its new height is given by the buoyancy force

$$F_B = gV(\rho(z + \delta z) - (\rho_{blob} + \delta\rho_{blob})). \quad (16)$$

Expand the density of the fluid in terms of  $z$

$$F_B = gV \left( \frac{\partial \rho}{\partial z} \delta z - \delta \rho_{blob} \right). \quad (17)$$

The fluid is neutrally stable if the force of buoyancy is zero.

$$\frac{\partial \rho}{\partial z} \delta z = \delta \rho_{blob} \quad (18)$$

The density is written as a function of  $T$  and  $P$ :

$$\rho = \rho(T, P) \quad (19)$$

$$\frac{\partial \rho}{\partial z} = \left( \frac{\partial \rho}{\partial T} \right)_P \frac{\partial T}{\partial z} + \left( \frac{\partial \rho}{\partial P} \right)_T \frac{\partial P}{\partial z} \quad (20)$$

Inserting this into Eq. 18 gives

$$\frac{\partial \rho_{blob}}{\partial z} = \left( \frac{\partial \rho}{\partial T} \right)_P \frac{\partial T}{\partial z} + \left( \frac{\partial \rho}{\partial P} \right)_T \frac{\partial P}{\partial z} \quad (21)$$

Using the momentum and adiabatic energy balance (heat transfer term is neglected) we obtain

$$\frac{\partial \rho_{blob}}{\partial z} = \frac{C_v \rho^2 \frac{\partial T}{\partial z}}{T \left( \frac{\partial P}{\partial T} \right)_\rho} \quad (22)$$

Simplifying and using some thermodynamic relations,

$$\left( \frac{\partial \rho}{\partial T} \right)_P \partial T z + \left( \frac{\partial \rho}{\partial P} \right)_T g \rho = \frac{C_v \rho^2 \frac{\partial T}{\partial z}}{T \left( \frac{\partial P}{\partial T} \right)_\rho} \quad (23)$$

$$\frac{\partial T}{\partial z} = \left( 1 - \frac{C_v}{C_P} \right) \left( \frac{\partial T}{\partial P} \right)_\rho \rho g \quad (24)$$

which is an expression for the adiabatic temperature gradient in terms of experimentally accessible quantities.

## 5. Governing Equations

The mass balance for an incompressible fluid is

$$\frac{\partial \rho}{\partial t} + \nabla \cdot (\rho v) = 0. \quad (25)$$

The Navier-Stokes equations contain the effects of viscosity due to compressibility.

$$\rho \left( \frac{\partial v}{\partial t} + (v \cdot \nabla) v \right) + \nabla P = \mu [\nabla^2 v + \frac{1}{3} \nabla (\nabla \cdot v)] + \rho g \hat{k} \quad (26)$$

The conservation of energy is a bit tricky, so I will derive it.

$$d\hat{U} = T d\hat{S} - P d\hat{V} \quad (27)$$

$$\hat{U} = \hat{U}(T, V) \quad (28)$$

$$d\hat{U} = \frac{\partial \hat{U}}{\partial T}_V dT + \frac{\partial \hat{U}}{\partial V}_T d\hat{V} \quad (29)$$

$$\frac{\partial \hat{U}}{\partial V}_T = T \frac{\partial \hat{S}}{\partial V}_T - P = T \frac{\partial P}{\partial T}_V - P \quad (30)$$

$$d\hat{U} = \hat{C}_V dT + (T \frac{\partial P}{\partial T}_V - P) d\hat{V} \quad (31)$$

$$\hat{C}_V dT = -T \frac{\partial P}{\partial T}_V d\hat{V} + T d\hat{S} \quad (32)$$

$$\rho C_V \frac{DT}{Dt} = -T \frac{\partial P}{\partial T}_V \nabla \cdot v + \nabla \cdot q + \mu \Phi \quad (33)$$

Inserting the van der Waals equation of state and the diverging thermal conductivity gives

$$C_v \rho \left( \frac{\partial T}{\partial t} + v \cdot \nabla T \right) = -(P + a\rho^2) \nabla \cdot v + k \nabla \cdot [(1 + \Lambda(T/T_c - 1)^{-1/2}) \nabla T] + \mu \Phi \quad (34)$$

where  $\Phi$  is given by:

$$\Phi = \left( \frac{\partial v_i}{\partial x_j} + \frac{\partial v_j}{\partial x_i} - \frac{2}{3} \delta_{ij} \nabla \cdot v \right) \frac{\partial v_i}{\partial x_j} \quad (35)$$

Recall the van der Waals equation of state

$$P = \frac{\mathfrak{R} \rho T}{1 - b\rho} - a\rho^2 \quad (36)$$

The parameters a and b are found from their values at the critical point, and  $\Lambda$  is given by [1]

$$a = \frac{9 T_c \mathcal{R}}{8 \rho_c} \quad (37)$$

$$b = \frac{1}{3\rho_c} \quad (38)$$

$$\Lambda = 3/4 \quad (39)$$

### 5.1. Boundary Conditions

Unlike incompressible convection, the amount of particles put into the cell needs to be specified. In order to avoid ever calculating an infinite pressure at  $\rho = 1/b$  set

$$\max(\rho) = \rho_{max} \quad (40)$$

as the boundary condition on the density.

The temperature is specified as a combination of temperature and flux. I follow [11] to match the flux and temperature at the solid - fluid interface. Focus just the bottom solid, the only difference in the top is that the z coordinate is flipped.

The energy balance in the solid is

$$C_{solid} \rho_{solid} \frac{\partial T_{solid}}{\partial t} = k_{solid} \nabla^2 T_{solid}. \quad (41)$$

The boundary condition at the interface is:

$$T_{solid} = T_{fluid} \quad (42)$$

$$k_{solid} \frac{\partial T_{solid}}{\partial z} = k_{fluid} \frac{\partial T_{fluid}}{\partial z}. \quad (43)$$

Expand  $T_{solid}$  as a static solution plus a deviation:

$$T_{solid} = T'_{solid} + \theta \quad (44)$$

Static solution for solid:

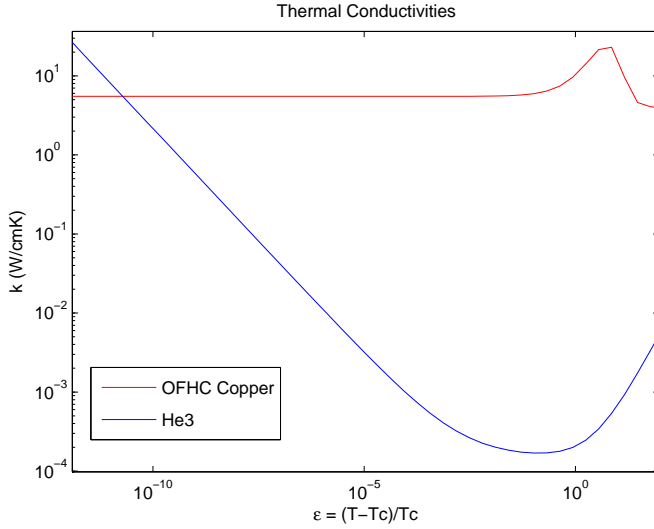


Fig. 3. Conductivity of  ${}^3\text{He}$  close to the critical point

$$T'_{solid} = T_{bottom} + \frac{k_{solid}}{k_{fluid}} z \quad (45)$$

Assume the solid plate is infinite and the disturbances decay at  $-\infty$ , then

$$C_{solid}\rho_{solid} \frac{\partial \theta}{\partial t} = k_{solid} \nabla^2 \theta \quad (46)$$

$$\Theta = \theta^{i l_x x + p t} \quad (47)$$

$$p \Theta = \frac{k_{solid}}{C_{solid}\rho_{solid}} \left( \frac{\partial^2}{\partial z^2} - l_x^2 \right) \Theta \quad (48)$$

$$\Theta = A_0 \exp \left[ z \sqrt{l_x^2 + p \frac{C_{solid}\rho_{solid}}{k_{solid}}} \right] \quad (49)$$

Recall the boundary conditions

$$k_{solid} \frac{\partial \theta}{\partial z} = k_{fluid} \frac{\partial \theta_{fluid}}{\partial z} \quad (50)$$

$$\theta = \theta_{fluid} \quad (51)$$

This can be solved for the fluid variables and rearranged to give

$$\frac{\partial \theta_{fluid}}{\partial z} = \frac{k_{solid}}{k_{fluid}} \sqrt{l_x^2 + p/\kappa} \theta_{fluid} \quad (52)$$

$$\frac{\partial \theta_{fluid}}{\partial z} = \frac{k_{solid}}{k_{fluid}} l_x \theta_{fluid} \quad (53)$$

If the thermal conductivity of the solid is much greater than that of the fluid, then using a constant temperature is a reasonable approximation. If the reverse is true, then a constant flux should be imposed.

It was noted earlier that the conductivity of the fluid goes to infinity as the critical point is approached; this initially led to the conclusion that all past theoretical work was incorrect. This was checked by looking up the conductivity of  ${}^3\text{He}$  in [14], and this is displayed in figure 3

The conductivities of some common materials are

$$k_{Copper} = O(1 - 100) \frac{W}{cm^\circ K} \quad (54)$$

$$k_{Steel} = O(0.01) \frac{W}{cm^\circ K} \quad (55)$$

$$k_{Kevlar} = O(10^{-6}) \frac{W}{cm^\circ K} \quad (56)$$

For experiments done by Kogan [12] copper was used, and for this the fixed temperature boundary (for which the critical Rayleigh number was found) is appropriate. It is assumed that the boundaries satisfy no-shear, whereas Kogan and others have used no-slip.

Boundary Conditions:

$$\frac{\partial T}{\partial z} \Big|_{(z=0)} = F_{bottom} \quad (57)$$

$$\frac{\partial T}{\partial z} \Big|_{(z=1)} = F_{top} \quad (58)$$

$$v_{z(z=0)} = v_{z(z=1)} = 0 \quad (59)$$

$$\frac{\partial v_x}{\partial z} \Big|_{(z=0)} = 0 \quad \frac{\partial v_x}{\partial z} \Big|_{(z=1)} = 0 \quad (60)$$

## 6. Dimensionless Equations

Because the Prandtl number goes to infinity, a thermal time scale is used. Let  $\tilde{t} = \frac{tk}{C_v \rho_c d^2}$ ,  $\tilde{T} = \frac{T}{T_c}$ ,  $\tilde{x} = \frac{x}{d}$ ,  $\tilde{\rho} = \frac{\rho}{\rho_c}$ ,  $\tilde{a} = \frac{a}{8}$  and  $\tilde{b} = 1/3$  where the tilde represents the dimensionless variables. Dropping the tilde we obtain the following dimensionless equations:

Mass Balance:

$$\frac{\partial \rho}{\partial t} + \nabla \cdot (\rho v) = 0 \quad (61)$$

Momentum Balance:

$$\rho \left( \frac{\partial v}{\partial t} + (v \cdot \nabla) v \right) + \nabla P = \sigma [\nabla^2 v + \frac{1}{3} \nabla (\nabla \cdot v)] + \sigma \lambda \rho \hat{k} \quad (62)$$

Energy:

$$\lambda m \rho \left( \frac{\partial T}{\partial t} + v \cdot \nabla T \right) = -(P + \lambda m (\gamma - 1) a \rho^2) \nabla \cdot v + \lambda m \nabla \cdot [(1 + \Lambda (T - 1)^{-1/2}) \nabla T] + \sigma \Phi \quad (63)$$

where  $\Phi$  is given by:

$$\Phi = \left( \frac{\partial v_i}{\partial x_j} + \frac{\partial v_j}{\partial x_i} - \frac{2}{3} \delta_{ij} \nabla \cdot v \right) \frac{\partial v_i}{\partial x_j} \quad (64)$$

Equation of state:

$$P = \lambda m (\gamma - 1) \left( \frac{\rho T}{1 - b \rho} - a \rho^2 \right) \quad (65)$$

Boundary Conditions:

$$\max(\rho) = \rho_{max} \quad (66)$$

$$\frac{\partial T}{\partial z} \Big|_{(z=0)} = F_{bottom} \quad (67)$$

$$\frac{\partial T}{\partial z(z=1)} = F_{top} \quad (68)$$

$$v_{z(z=0)} = v_{z(z=1)} = 0 \quad (69)$$

$$\frac{\partial v_x}{\partial z(z=0)} = \frac{\partial v_x}{\partial z(z=1)} = 0 \quad (70)$$

where the dimensionless parameters are given by

$$\sigma = \frac{\mu C_v}{k} \quad (71)$$

$$\lambda = \frac{g C_v d^3 \rho_c^2}{\mu k} \quad (72)$$

$$m = \frac{C_v^2 T_c \mu}{k g d} \quad (73)$$

$$\gamma - 1 = \frac{\mathcal{R}}{C_v} \quad (74)$$

Notice that the right hand side of the equation of state could have used a much simpler expression, this one was chosen so that when a perturbation method solution is done such that  $\lambda$  was expanded then the first order deviation of  $\lambda$  would drop out of the first order equations.

## 7. Onset of Convection

### 7.1. Scaling

Hurle shows that as the thermal conductivity of the fluid over the conductivity of the solid goes to infinity, the wavenumber of the least unstable mode is zero. Because the convection cell is much wider than it is high, let

$$x = \epsilon^{-1/2} \zeta \quad (75)$$

$$t = \epsilon^{-2} \tau \quad (76)$$

where the time scaling is the standard one and I do not know what motivates it.

Because conservation of volume might dominate when convection starts, it is suggestive to scale the x and z velocities as

$$u = \epsilon^{1/2} U \quad (77)$$

$$w = \epsilon W \quad (78)$$

Expand the variables as follows:

$$\rho = \rho_s + \epsilon \rho_1 + \epsilon^2 \rho_2 + \dots \quad (79)$$

$$T = T_s + \epsilon T_1 + \epsilon^2 T_2 + \dots \quad (80)$$

$$P = P_s + \epsilon P_1 + \epsilon^2 P_2 + \dots \quad (81)$$

$$U = U_s + \epsilon U_1 + \epsilon^2 U_2 + \dots \quad (82)$$

$$W = W_s + \epsilon W_1 + \epsilon^2 W_2 + \dots \quad (83)$$

### 7.2. Order 1 (Static Solution)

$$\frac{\partial P_s}{\partial \zeta} = 0 \quad (84)$$

$$\frac{\partial P_s}{\partial z} = \sigma \lambda \rho_s \quad (85)$$

$$0 = \frac{\partial}{\partial z} \left[ (1 + \Lambda(T_s - 1)^{-1/2}) \frac{\partial T_s}{\partial z} \right] \quad (86)$$

$$P_s = \lambda m (\gamma - 1) \left( \frac{\rho_s T_s}{1 - b\rho_s} - a\rho_s^2 \right) \quad (87)$$

Order one boundary conditions:

$$\frac{\partial T_s}{\partial z} \Big|_{z=0} = F_{bottom} \quad (88)$$

$$\frac{\partial T_s}{\partial z} \Big|_{z=1} = F_{top} \quad (89)$$

$$\max(\rho_s) = \rho_{max} \quad (90)$$

The temperature profile has an analytic profile

$$T_s = c_1 z + c_2 + 2\Lambda^2 - 2\Lambda(c_1 z + c_2 + \Lambda^2 - 1)^{1/2} \quad (91)$$

The density and pressure profiles are solved numerically

$$\left( \frac{T_s}{1 - b\rho_s} + \frac{bT_s\rho_s}{(1 - b\rho_s)^2} - 2a\rho_s \right) \frac{d\rho_s}{dz} = \left( \frac{\sigma}{(\gamma - 1)m} - \frac{1}{1 - b\rho_s} \frac{dT_s}{dz} \right) \rho_s \quad (92)$$

$$P_s = \frac{\rho_s T_s}{1 - b\rho_s} - a\rho_s^2 \quad (93)$$

The temperature profile is shown in Figure 4 for an artificial case.  $\Lambda = 0$  is what is used for ideal gases and far away from the critical point, and  $\Lambda = 10$  is a fluid strongly effected by deviations close to the critical point.

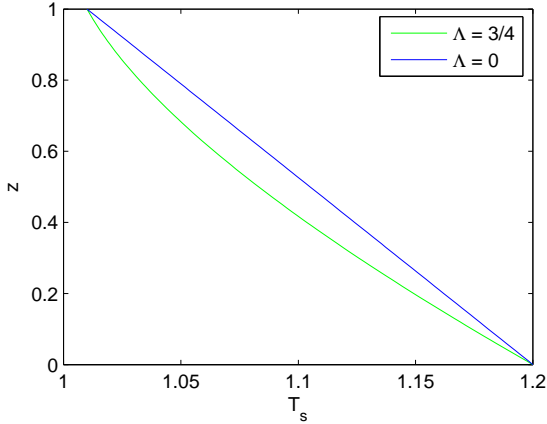


Fig. 4. Static Temperature Profile. The addition of the the Lambda effects cause the temperature profiles to be nonlinear

The pressure and the density profiles are shown in Figures 5 and 6 respectively. The effects of the van der Waals gas can easily seen from the pressure profiles. Increasing the attraction parameter decreases the pressure, whereas increasing the size of the hard spherical particles causes the pressure to increase. These effects cause the differences in the density profiles.

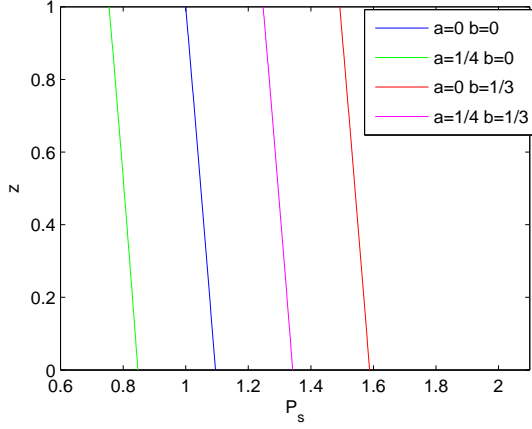


Fig. 5. Static Pressure Profile. The addition of the attractive force  $a$ , reduces the pressure, whereas the repulsive forces  $b$  cause the pressure to increase. A combination of the two is the linear sum of the two effects.

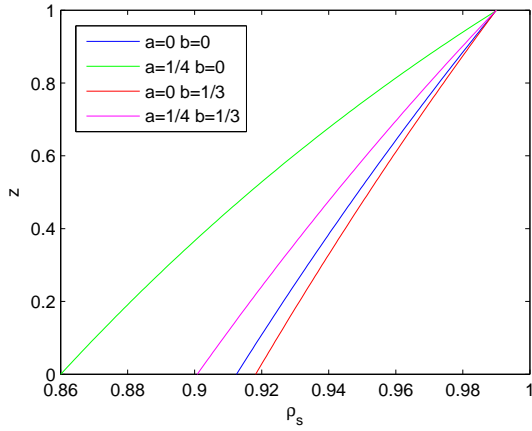


Fig. 6. Static Density Profile. The adverse temperature gradient causes the fluid at the bottom to be less dense than the fluid above it. Clearly this is an unstable situation.

### 7.3. Order $\epsilon$

The governing equations at order  $\epsilon$  give:

$$0 = \rho_s \frac{\partial U_1}{\partial \zeta} + \rho_s \frac{\partial W_1}{\partial z} + W_1 \frac{\partial \rho_s}{\partial z} \quad (94)$$

$$\frac{\partial P_1}{\partial \zeta} = \sigma \frac{\partial^2 U_1}{\partial z^2} \quad (95)$$

$$\frac{\partial P_1}{\partial z} = \sigma \lambda \rho_1 \quad (96)$$

$$0 = \frac{\partial}{\partial z} \left[ (1 + \Lambda(T_s - 1)^{-1/2}) \frac{\partial T_1}{\partial z} - \frac{1}{2} \Lambda(T_s - 1)^{-3/2} T_1 \frac{\partial T_s}{\partial z} \right] \quad (97)$$

$$P_1 = \lambda m (\gamma - 1) \left( \frac{\rho_1 T_s}{(1 - b\rho_s)^2} + \frac{\rho_s T_1}{1 - b\rho_s} - 2a\rho_s \rho_1 \right) \quad (98)$$

The order  $\epsilon$  boundary conditions are:

$$W_1(z=0) = W_1(z=1) = 0 \quad (99)$$

$$\left(\frac{\partial U_1}{\partial z}\right)_{(z=0)} = \left(\frac{\partial U_1}{\partial z}\right)_{(z=1)} = 0 \quad (100)$$

$$\left((1 + \Lambda(T_s - 1)^{-1/2})\frac{\partial T_s}{\partial z} - \frac{1}{2}\Lambda(T_s - 1)^{-3/2}T_1\frac{\partial T_1}{\partial z}\right)_{(z=0)} = 0 \quad (101)$$

$$\left((1 + \Lambda(T_s - 1)^{-1/2})\frac{\partial T_s}{\partial z} - \frac{1}{2}\Lambda(T_s - 1)^{-3/2}T_1\frac{\partial T_1}{\partial z}\right)_{(z=1)} = 0 \quad (102)$$

The solution to these equations is given by

$$T_1 = \frac{f(\zeta, \tau)}{1 + \Lambda(T_s - 1)^{-1/2}} = f(\zeta, \tau)g_1 \quad (103)$$

$$\rho_1 = f(\zeta, \tau)g_2 \quad (104)$$

$$P_1 = \lambda m(\gamma - 1)f(\zeta, \tau)g_3 \quad (105)$$

$$U_1 = \frac{\lambda m(\gamma - 1)}{\sigma} \frac{\partial f(\zeta, \tau)}{\partial \zeta} g_4 \quad (106)$$

$$W_1 = \frac{\lambda m(\gamma - 1)}{\sigma} \frac{\partial^2 f(\zeta, \tau)}{\partial \zeta^2} g_5 \quad (107)$$

where  $g_2$  through  $g_5$  are given by

$$\left(-\frac{\sigma}{m(\gamma - 1)} + \frac{d}{dz} \left(\frac{T_s}{(1 - b\rho_s)^2} - 2a\rho_s\right)\right) g_2 + \left(\frac{T_s}{(1 - b\rho_s)^2} - 2a\rho_s\right) \frac{dg_2}{dz} = -\frac{d}{dz} \left(\frac{\rho_s g_1}{1 - b\rho_s}\right) \quad (108)$$

$$g_3 = \frac{g_2 T_s}{1 - b\rho_s} + \frac{\rho_s g_1}{1 - b\rho_s} - 2a\rho_s g_2 \quad (109)$$

$$\frac{d^2 g_4}{dz^2} = g_3 \quad (110)$$

$$\frac{dg_5}{dz} + \frac{1}{\rho_s} \frac{d\rho_s}{dz} g_5 = -g_4 \quad (111)$$

with boundary conditions

$$g_5(z=0) = g_5(z=1) = 0 \quad (112)$$

$$\left(\frac{dg_4}{dz}\right)_{(z=0)} = \left(\frac{dg_4}{dz}\right)_{(z=1)} = 0 \quad (113)$$

where the functions  $g_2$  through  $g_5$  are found numerically. The boundary value problems are solved using the shooting method. Integrating across the  $z$  domain, the x-component momentum equation gives the condition that

$$\int_0^1 g_3 dz = 0. \quad (114)$$

This trick makes the problem substantially easier, instead of shooting in two directions at the same time, first an iterative method is used to find  $g_2(z=0)$  and once this solution is obtained an independent shooting method is used to obtain the value of  $g_4(z=0) = 0$  that matches  $g_5(z=1) = 0$ .

For  $\frac{T-T_c}{T_c} = 0.01$  and  $\rho_{max} = 0.99$  the horizontal and vertical velocities are shown in Figures 7 and 8

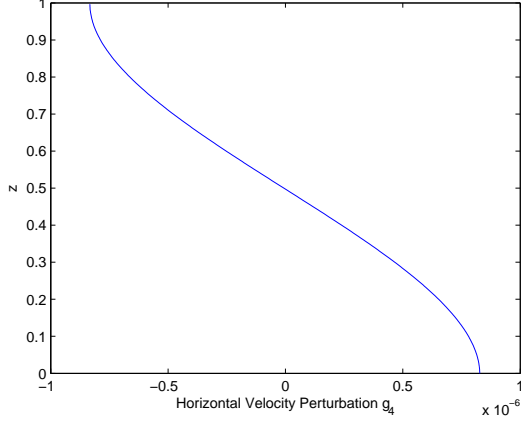


Fig. 7. Horizontal Perturbation Velocity

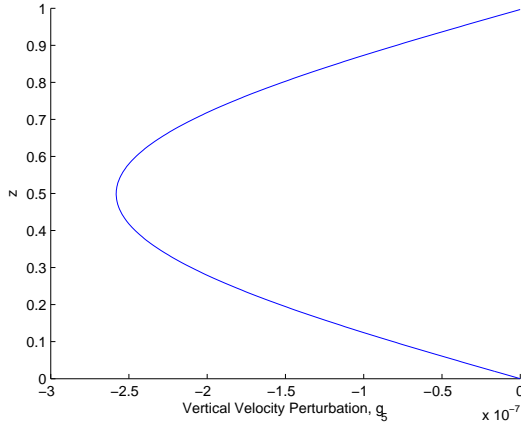


Fig. 8. Vertical Perturbation Velocity

#### 7.4. Order $\epsilon^2$

Only the heat equation is necessary, this is

$$\lambda m \rho_s W_1 \frac{\partial T_s}{\partial z} = - (P_s + \lambda m (\gamma - 1) a \rho_s^2) \left( \frac{\partial U_1}{\partial \zeta} + \frac{\partial W_1}{\partial z} \right) + \lambda m \left[ 1 + \Lambda (T_s - 1)^{-1/2} \right] \frac{\partial^2 T_1}{\partial \zeta^2} + \frac{\partial q}{\partial z} \quad (115)$$

Inserting the order  $\epsilon$  solution and integrating from 0 to 1 eliminates the flux in the z-direction. It is seen that  $\frac{\partial^2 f}{\partial \zeta^2}$  is in front of all the terms so this cancels.

$$0 = \int_0^1 \left[ \frac{\lambda m (\gamma - 1)}{\sigma} g_5 \rho_s \frac{\partial T_s}{\partial z} + \frac{(\gamma - 1)}{\sigma} (P_s + \lambda m (\gamma - 1) a \rho_s^2) \left( g_4 + \frac{\partial g_5}{\partial z} \right) - 1 \right] dz \quad (116)$$

The expression is then simplified using the order  $\epsilon$  governing equations.

$$\frac{\lambda m (\gamma - 1)}{\sigma} \int_0^1 g_5 \left[ \rho_s \frac{\partial T_s}{\partial z} - \frac{(\gamma - 1) T_s}{1 - b \rho_s} \frac{\partial \rho_s}{\partial z} \right] dz = 1 \quad (117)$$

The equivalent expression

$$\frac{\lambda m(\gamma - 1)}{\sigma} \int_0^1 g_5 \rho_s \left[ \frac{\partial T_s}{\partial z} - \frac{(\gamma - 1) T_s}{1 - b \rho_s} \frac{\partial \ln(\rho_s)}{\partial z} \right] dz = 1 \quad (118)$$

is sometimes preferred.

For an experimentalist the difference in top and bottom temperatures was calculated for a given temperature of the bottom plate. For a fixed density of  $\rho_{max} = 0.99$ , with heat conductivity from [14], heat capacity from [3], and viscosity from [16] this is shown in Figure 9

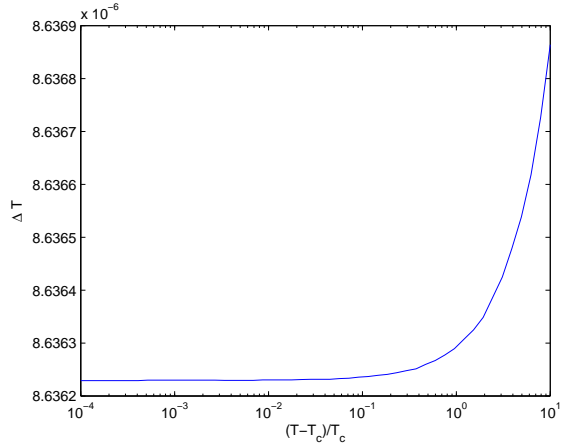


Fig. 9.

Figure 9 can be compared with Figure 2 in Kogan et. al [12]. Kogan used He3 for constant temperature and no slip walls. The magnitude of the  $\Delta T$  close to the critical point for the simulation is about  $20 \mu K$  whereas the experimental value is closer to  $4 \mu K$ . The slope of the plot as curve further away from the critical point is also much shallower than that shown in [12], but this depends highly on the value of viscosity, heat capacity, and conductivity; none of which were divulged in the paper by Kogan.

## 8. Conclusion

A criterium for the onset of convection for a van der Waals fluid was found. It is an average over the cell of the Rayleigh and Schwarzschild criteria. Numerical solutions have some similarities with experimental data, but are far from quantitative. The boundary conditions used were constant flux, although most experiments done so far have been justified in their use of constant temperature, so this work predicts the onset of convection for a situation with walls made of a low conducting material, such as kevlar. Interesting aspects of this problem that require further work involve finding the evolution equation for this situation, to see if any patterns occur that are previously unknown. It would also be interesting to move away from the critical point and try to model two different phases.

## References

- [1] Amiroudine, S., Bontoux, P., Larroude, P., Gilly, B., Zappoli, B. 2001 Direct numerical simulation of instabilities in a two-dimensional near-critical fluid layer heated from below. J. Fluid Mech. **442**, 119-140.
- [2] Assenheimer, M. and Steinberg, V. 1993 Rayleigh Benard Convection near the Gas-Liquid Critical Point. Phys. Rev. Let. **70**, 3888-3891.
- [3] Brown, G. R., and Meyer, H. 1972 Study of the Specific-Heat Singularity of  $He^3$  near Its Critical Point. Phys. Rev. A. **6**, 364-377.

- [4] Callen, H. B. 1985 Thermodynamics and an introduction to Thermostatistics, 2nd Ed. Wiley and Sons.
- [5] Carles, P. 2000 The onset of free convection near the liquid-vapour critical point Part 2: Unsteady heating. *Physica D.* **147**, 36-58.
- [6] Carles, P. and Ugurtas, B. 1999 The onset of free convection near the liquid-vapour critical point Part 1: Stationary initial state. *Physica D.* **126**, 69-82.
- [7] Chapman, C. J. and Proctor, M. R. E. 1980 Nonlinear Rayleigh-Benard convection between poorly conducting boundaries. *J. Fluid Mech* **101**, 759-782.
- [8] Depassier, M. C. and Spiegel, E. A. 1981 The Large-scale structure of compressible convection. *Astro. J.* **86**, 496-512.
- [9] El Khouri, L. and Carles, P. 2002 Scenarios for the onset of convection close to the critical point. *Phys. Rev. E.* **66**, 066309 1-4.
- [10] Gitterman, M. 1978 Hydrodynamics of fluids near a critical point. *Rev. of Mod. Phys.* **50**, 85-106.
- [11] Hurle, D. T. J., Jakeman, E., and Pike, E. R. 1967 On the solution of the Benard problem with boundaries of finite conductivity. *Proc. Roy. Soc. A* **296**, 469-475.
- [12] Kogan, A. B., Murphy, D., and Meyer, H. 1999 Rayleigh-Benard Convection Onset in a Compressible Fluid:  ${}^3\text{He}$  near  $T_c$ . *Phys. Rev. Let.* **82**, 4635-4638.
- [13] Onuki, A., Hao, H., and Ferrell, R. A. 1990 Fast adiabatic equilibration in a single-component fluid near the liquid-vapor critical point. *Phys. Rev. A.* **41**, 2256-2258.
- [14] Pittman, C. E., Cohen, L. H., and Meyer, H. 1982 Transport Properties of Helium Near the Liquid-Vapor Critical Point. *J. low Temp. Phys.* **46**, 115-135.
- [15] Polezhaev, V. I. and Soboleva, E. B. 2004 Rayleigh-Benard Convection in a Near-Critical Fluid in the Neighborhood of the Stability Threshold. *Fluid Dynamiv.* **40**, 209-220.
- [16] Taylor, R. D. and Dash, J. G. 1957 Hydrodynamics of Oscillating Disks in Viscous Fluids: Viscosities of Liquids  $\text{He}^3$  and  $\text{He}^4$ . *Phys. Rev.* **106**, 398-403.